

## MODELLING CROP GEOMETRY USING MULTIPLE VIEW ANGLES

O.W. VONDER\*, J.G.P.W. CLEVERS\*, J.F. DESPRATS\*\*, C. KING\*\*,  
L. PRÉVOT\*\*\*, N. BRUGUIER\*\*\*

\* Centre for Geo-Information, Wageningen-UR, The Netherlands

[oscar.vonder@staff.girs.wag-ur.nl](mailto:oscar.vonder@staff.girs.wag-ur.nl)

[jan.clevers@staff.girs.wag-ur.nl](mailto:jan.clevers@staff.girs.wag-ur.nl)

\*\* BRGM, Orléans, France

\*\*\* INRA, Avignon, France

Working Group TC VII/2

**KEY WORDS:** Agriculture, Biomass, Calibration, Data dissemination, Modelling, Monitoring, Validation

### ABSTRACT

A simple canopy reflection model (Crop Geometry Interaction) was built based on linear mixing and viewing geometry. Such a model in combination with the SAIL model could improve our knowledge on crop growth in the early stages of the season. This enables us to adjust SVAT models early in the growth season. The CGI model was calibrated using winter wheat field measurements in combination with a large amount of airborne near infrared POLDER images obtained during the ReSeDA experiment at the Alpilles test site in Southern France from October 1996 to November 1997. Simulating (empirical) crop growth parameters such as LAI, coverage and height were combined with simulated sun angles and fed to SAIL and a combined CGI/SAIL model. Calibration of the canopy reflection models shows good results.

### 1 INTRODUCTION

The main objective of the European project ReSeDA is the use of multi-sensor and multi-temporal observations for monitoring soil and vegetation processes, in relation with the atmospheric boundary layer at local and regional scales by assimilation of remote sensing data into canopy and soil functioning models (Prevot et al., 1998). As member in the ReSeDA project the Centre for Geo-Information is investigating the role of viewing angles in the prediction of leading crop geometry parameters such as crop height, crop diameter and crop cover percentage. A simple canopy reflection model (Crop Geometry Interaction) is being built based on linear mixing and viewing geometry. In combination with the SAIL model it is expected to predict some of the parameters used in the models studied by other partners in the ReSeDA project. It is hoped to predict crop cover percentage (input for the models Isba and Isba A-gs), crop height (input for SiSPAT, AliBi and CLOUD1) and diameter before crop closure.

Depending on the view angle, crop diameter, plant distance, row distance and crop height only part of a single plant can be seen by the sensor. By using multiple view angles it may be possible to predict some of the plant geometry parameters such as height, diameter and crop coverage. To reduce costs, using as few view angles as possible would be the ideal situation. There are two view angles where the calculation of the geometry is similar, namely from nadir and in the hotspot. In both situations part of the soil is blocked either by the side column of the crop or by the shadow of the crop. In the case of the hotspot, total reflection can be built from sunlit crop reflection and sunlit soil reflection. In the geometry model no difference will be made between top and side reflection of the crop. In the second case (nadir), total reflection can be built from sunlit soil, shadowed soil and sunlit crop reflection. Especially the stage before crop closure is being studied because then soil reflection will contribute much to total reflectance. In order to calibrate the model use will be made of the field measurements done on the ReSeDA test site near Avignon, France in June 1997. The measurements contain nadir photographs and field observations on crop height and diameter. For validation use will be made of field measurements performed by BRGM and INRA, and airborne imagery of the POLDER instrument. POLDER has been mounted on an aeroplane, which passed the ReSeDA test site on 16 days during the growing season of 1997. A total of almost 1200 raw images (each with 9 bands) with a pixel size of 20x20m were gathered during this period. The raw images were atmospherically corrected and geocoded by CESBIO. Because of the wide field-of-view each pixel inside these images has a different viewing angle.

Near infrared wheat reflection (nadir and hotspot) measured by the POLDER instrument will be simulated using SAIL, CGI and wheat field measurements from the ReSeDA test site. Nadir and hotspot views were chosen because they have a lot in common. Infrared reflection was chosen because shadowing of vegetation has larger influence on total reflection in the infrared than in the visible bands.

## 2 CANOPY REFLECTION MODELLING

### 2.1 Introduction

A simple model (CGI) was built based on the principles described by Rosema et al. (1992) in the Forest Light Interaction Model. According to Rosema et al.(1992) and Nilson and Peterson (1991) the Suits/SAIL models were found to be disturbed by a strong influence of the understory (soil or vegetation), especially when the LAI of the understory reaches values higher than 1. Also clumsiness, open spots and shadowing are not accounted for in the models. So Rosema et al.(1992) developed a model based on the following principals. Viewing a forest from an aeroplane means that we are looking at two basic parameters: Forest, and Ground (bare soil or understory). These two parameters are both influenced by the place of the sun and the viewing angle. This makes it possible to differ four parameters:

Sunlight Forest (Fb)	Sunlight Ground (Sb)
Shadowed Forest (Fd)	Shadowed Ground (Sd)

Where:  $Total\ area = Fb + Fd + Sb + Sd$  (1)

By multiplying each fraction with their directional reflectance gives us the total reflection as seen by the instrument. Calculations of the fractions by Rosema et al. were based on circular crops. However, the CGI model will be based on a simplified crop represented by a square column. Geometry using square columns can easily be calculated using triangular expressions.

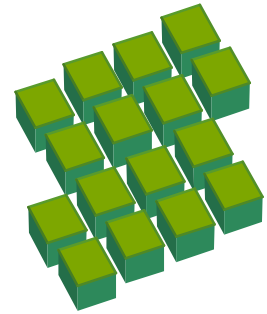


Figure 1: Hotspot viewing

### 2.2 Geometric Modelling

In this section we will try to calculate which part of the plant is visible under different view angles. Therefore we need to set some parameters. Zenith angle (Z) is the off-nadir viewing angle, where 0 is nadir. Azimuth angle (A) is the azimuth view angle towards the row. When looking straight in the row, azimuth will be 0 and perpendicular to the row, azimuth will be 90 degrees. To keep things simple we assume that a single plant is only affected by the nearest neighbour plants. We differentiate the following nearest neighbour plants; row neighbours, cross row neighbours and cross row corner neighbours. In the following sections the calculation of the component projections will be explained. First we will calculate the component fractions of a hotspot view, then the components of a nadir view where shadow will be calculated.

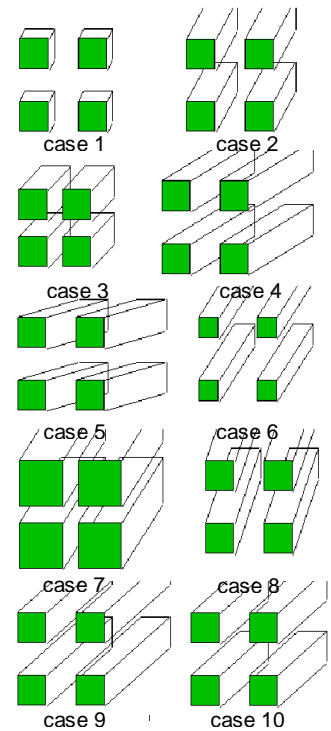


Figure 2: 10 Modelling Cases

### 2.3 Sunlit Bare Soil When Seen From the Hotspot

Hotspot viewing can be visualised as shown in figure 1. Depending on the view angle, crop diameter (dia) plant distance (dis), row distance (row) and crop height (H), only part of a single plant can be seen. When seen from nadir every crop has  $(dis \cdot row) - dia^2$  fraction bare soil before crop closure. However, with an off-nadir view angle part of this bare soil can not be seen because the crop blocks it. Instead we will see some side parts of the crops. The blocking part can be separated into two parts; one above and one aside the plant. However, in the case that a blocking part projection exceeds the space between two crops, part of the neighbour crop will be blocked. Other than in the model of Rosema et al., we assume for the geometry model that the top and side parts of a crop reflect the same way.

### 2.4 Sunlit and Shadowed Soil When Viewed From Nadir

Similar to the calculations of the visible sunlit bare soil area when looking from the hotspot are the calculations of the shadowed soil and vegetation components. If we are looking from nadir and assume a homogeneous crop height, shadowed top crop area is not present. So there will be three components left, sunlit top crop area (dark green), sunlit bare soil (light yellow) and shadowed bare soil (grey).

In general 10 cases can be distinguished in the CGI model (see figure 2). Based on the crop height, crop diameter and plant/row distances, shadowing/blocking exceeds the space of the neighbour crop in some cases (7,8 and 9). Those areas are being neglected. When simulating crop reflectance using the CGI model, viewing fractions (sunlit soil ( $Sf_s$ ), crop ( $Cf$ ) and shadowed soil ( $Sf_d$ )) are being calculated based on the modelling case they belong to.

## 2.5 Linear Mixing

Total reflectance (Tr) is built from the reflectance of its components (crop (Cr), sunlit soil (Sr<sub>s</sub>) and shadowed soil (Sr<sub>d</sub>)). With the geometry module of the CGI model we have calculated the fraction of each component. So:

$$Tr = (Cf * Cr) + (Sf_s * Sr_s) + (Sf_d * Sr_d) \quad (2)$$

There is no shadow seen when the view angle is equal to the sun zenith angle, and azimuth angles are also equal. In that case shadowed soil cover percentage = 0.

## 2.6 Multidirectional Reflection

The geometry model uses one value for the crop reflection. However, crop reflection shows directional behaviour so crop reflection will be simulated using the SAIL model. One of the parameters of SAIL is the LAI value. LAI is the amount of leaf (m<sup>2</sup>) per m<sup>2</sup>. For example, a single (square) plant on a square meter with one leaf layer and a diameter of 10 cm has a LAI of (0.10x0.10)/1 = 0.01. When calculating crop reflection with the SAIL model, SAIL will use a 1 % contribution of the crop and a 99% contribution of sunlit soil. In the CGI model, crop coverage is based on the crop diameter, which means that there is at least 1 leaf layer or more. In other words, the LAI we will use in SAIL as contribution to the CGI model can never be smaller than 1. So, crop reflection is being calculated with the SAIL module with an adjusted LAI called Plant<sub>LAI</sub>. Where Plant<sub>LAI</sub> = LAI / Cf.

Soils show also directional reflectance behaviour. Directional soil reflectance is calculated in the CGI model using a linear relation between the nadir bare soil reflectance (Sr<sub>n</sub>) and hotspot bare soil reflectance (Sr<sub>h</sub>).

## 2.7 Hotspot Error Correction

Measuring exactly in the hotspot is very difficult. However, slight changes have large effects on the total reflection properties especially with small, long crops such as wheat. Instead of only illuminated soil and illuminated crop, we will detect shadowed soil too. This effect increases with increasing crop height as is shown in the figure 3. So to compensate for this effect we assume in the model an error that increases with crop height. Without compensation the model calculates hotspot reflection in the following way:

$$Tr = (Sr_h * Sf_s) + (Cr_h * Cf_{top}) + (Cr_h * Cf_{side}) \quad (3)$$

Where Cf<sub>top</sub> = Crop top area fraction (equal to dia<sup>2</sup>)

and Cf<sub>side</sub> = Visible crop side area fraction

and Cr<sub>h</sub> = Crop hotspot reflectance

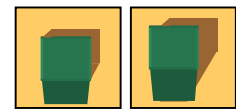


Figure 3: Hotspot error

We introduce the hotspot error area (Hf<sub>e</sub>):

$$Hf_e = (\text{height} / \text{dia}) * 0.1 * Cf_{side} \quad (4)$$

Where we assume a 10 % error to begin with, which grows when the height becomes larger than the diameter. However, this hotspot error area can never be larger than the sunlit soil area. The hotspot error area is subtracted from the total visible sunlit bare soil:

$$\text{Corrected } Sf_s = Sf_s - Hf_e \quad (5)$$

Which may never be a negative number! Now we calculate the reflection again:

$$Tr = (Sr_h * (Sf_s - Hf_e)) + (Cr_h * Cf_{top}) + (Cr_h * Cf_{side}) + (Sr_d * Hf_e) \quad (6)$$

This will decrease hotspot reflection for near nadir sun zenith angles in combination with crops where the crop height exceeds the crop diameter enormously.

## 2.8 Assumptions and Summary

Summarised, the CGI model combines directional reflectance (simulated using SAIL) with viewing geometry using linear mixing. The geometric model calculates the visible fractions of sunlit soil, shadowed soil, sunlit vegetation and shadowed vegetation for nadir and hotspot views. As an example figure 4 shows the contribution of the objects to total reflections as simulated for wheat field 300 of the ReSeDA test site.

Inputs are:

- Plant and row distance
- Crop diameter

- Crop height
- Crop (directional) reflectance
- Soil (directional) reflectance
- Shadowed (directional) soil reflectance

Assumptions:

- The crops are homogeneous in height, diameter and plant / row distance.
- To keep the model simple, crops are assumed to be square columns.
- Shadowing of the crop in the near infrared, caused by the instrument when viewing from the hotspot, does hardly reduce reflectance because of transmission and multiple scattering.
- Total reflection is built up from three components: sunlit soil, sunlit vegetation and shadowed soil.

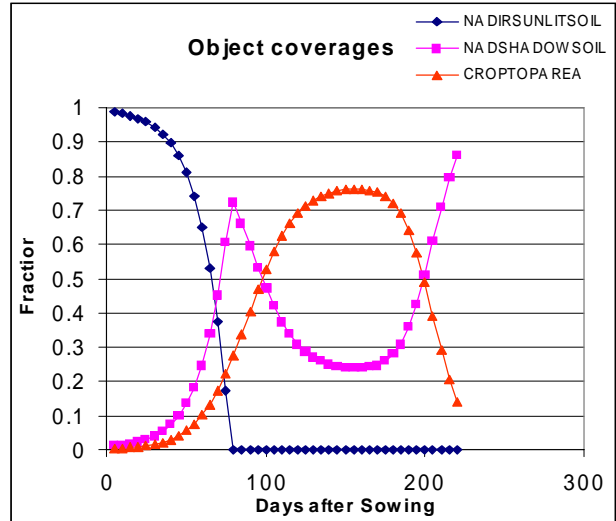


Figure 4: Simulated object fractions with CGI

### 3 WHEAT GROWTH SIMULATIONS

#### 3.1 Introduction

For the reflection simulation of the POLDER instrument with SAIL and CGI, crop growth will be simulated based on the actual field measurements of the ReSeDA test site 1997.

#### 3.2 Crop Height

Figure 5 presents the crop height measurements (destructive) of winter wheat at field 120. The decreasing crop height can be explained by the bending of the wheat head during maturation. Crop height in the CGI model will be simulated using a logistic model.

$$\text{Height} = (a / (1 + b * \text{Exp}(-c * \text{DaS}))) + 1 \quad (7)$$

Where:

Height = crop height in cm

a,b,c = parameters

DaS = Days after Sowing

For field 120 the following variables were found:

a = 80.34 (maximum crop height)

b = 700

c = 0.051



Figure 5: Measured versus simulated crop height.

In figure 5 you find the results of a season simulation using the logistic model and the parameters above.

#### Decreasing crop height

In the near infrared dried leaves reflect more than normal leaves and 10 leaves stacked together reflect more than 1 leaf (Buiten and Clevers, 1993 p. 94). Those effects cause the changes in near infrared reflectance during a growing season. Starting with healthy vegetation, reflection will increase because of the growing volume (LAI). When wheat matures, leaves contain less moisture, which also increases the reflection in the near infrared. So you would assume that near infrared reflection only increases during the growing season. However, for nadir images we see that infrared wheat reflection decreases at the end of the season. One

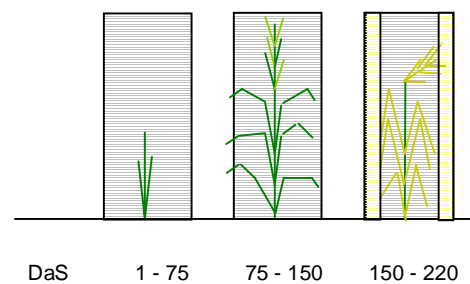


Figure 6: Crop architecture

explanation could be the changing architecture of the plant. During the maturing phase the drying leaves and the crop head bend sharply and the plant reduces in diameter and height.

When seen from the hotspot, the bending of the head decreases the crop height and diminishes the visible crop area as can be seen in figure 7. Early in the morning this effect has less influence on the hotspot reflection because hotspot measurements with low sun angles show hardly any bare soil. Depending on the height of the crop and the plant distance this effect becomes larger when the sun/hotspot angle reaches nadir. This effect is best simulated with decreasing crop height starting at some point during the growing season. To simulate the decrease in crop height at the end of the season it was chosen to run the logistic function until maximum crop height has been reached. Then maximum crop height is reduced linearly with a adjustable variable (Hc) over the remainder of the season ( $Height_{(LD \rightarrow Season)} = a - ((Hc / (season - LD)) * (DaS - LD))$ ). Where LD stands for the day after sowing at which the logistic model reaches the maximum crop height (a). Results are presented in figure 5 as “Logistic adjusted”.

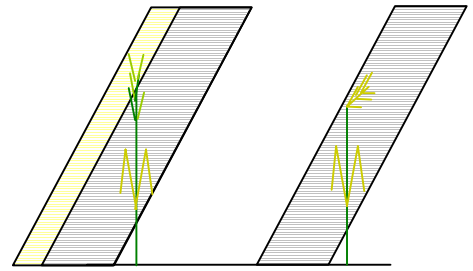


Figure 7: Bending crop heads

### 3.3 Leaf Area Index

One of the project partners (INRA) modelled the measured green LAI for the ReSeDA test site using the following function:

$$LAI(t) = M * (GRO(t) - SEN(t)) \quad (8)$$

Where :  $GRO(t) = 1 / (1 + \exp(-a * (t - t_i)))$  (9)

$$SEN(t) = 1 / (1 + \exp(-b * (t - t_s))) \quad (10)$$

For the simulation of wheat field 300 (see figure 8) we used:

t = time (days after sowing)

M = 2.5 (maximum LAI)

A = 0.06426

T<sub>i</sub> = 100 (LAI breakpoint)

B = 0.2

T<sub>s</sub> = 0.9 \* season

Season = 200 (days)

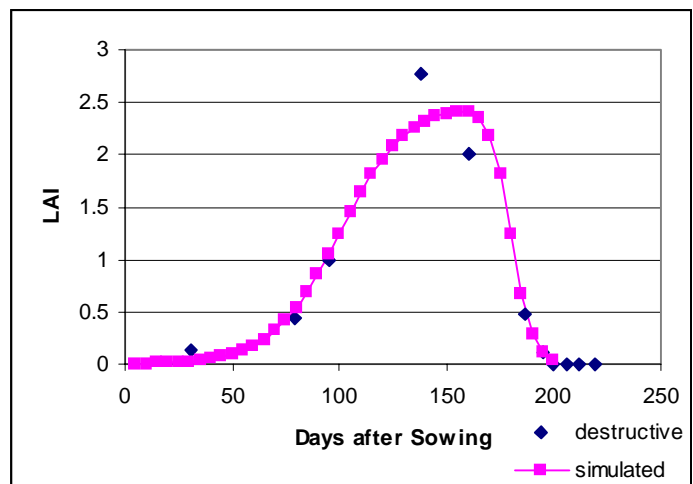


Figure 8: Measured versus modelled LAI for wheat field 300 of the ReSeDA test site (1997)

### 3.4 Crop Coverage

Crop coverage (C<sub>f</sub>) was estimated using “Dutch” relations between LAI and crop coverage for wheat (Bouman et al., 1992):

$$C_f = (1 - \exp(-a * LAI)) \quad (11)$$

According to Dutch measurements:

a = 0.6 (maximum coverage).

### 3.5 Soil Reflectance

Directional reflectance of bare soil was observed over the ReSeDA site with the POLDER instrument. Although there are various theoretical directional soil reflectance models (Jacquemoud et al, 1992), directional soil reflectance is calculated in the CGI model using a linear relation between the nadir bare soil reflectance (S<sub>r<sub>n</sub></sub>) and hotspot bare soil reflectance (S<sub>r<sub>h</sub></sub>) (see figure 9).

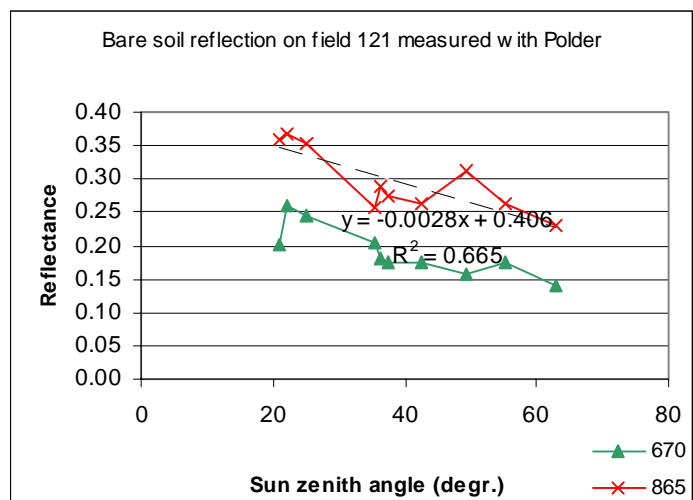


Figure 9: Measured versus modelled bare soil reflectance

$$Sr_n = Sr_h - \text{Sun zenith angle} * a \tag{12}$$

Where a and Sr<sub>h</sub> were empirically determined.

a = Directional sensitivity (0.0028 for field 121)

Sr<sub>h</sub> = Soil reflection when measured from the hotspot (0.406 for field 121)

This simple function will be used to adjust dynamically the soil reflection in the CGI and SAIL model.

### 3.6 Wheat Leaf Reflectance

The leaf reflectance and transmittance is used as input for the SAIL model to calculate total crop reflection. Figure 10 shows wheat leaf reflectance and transmittance that were used in the CGI and SAIL simulations.

### 3.7 Rainfall

During the data collection period a weather station (Meteo France) was installed at the test site. Because there was hardly any rainfall during the extreme dry growing season of 1997, no difference was made between dry and wet soils during the growing season.

### 3.8 Leaf Angle Distribution

Crop leaf angle properties of wheat change during the season. In the first weeks, when the crop just appears on the surface, wheat leaves will have an almost vertical leaf angle distribution. Then when the crop grows, it approaches a more spherical distribution. Finally in the last and yellowing phase of wheat, leaves bend sharply because of drying. When simulating crop reflection with the SAIL model you can choose between 12 leaf angle distribution functions given by the model or create your own. The three stages as described above can be simulated using the LIDF groups 9,2 and 7 of the SAIL model (Verhoef & Bunnik, 1981). However when simulating a complete wheat season we have to switch smoothly between those groups. So in the CGI model the linear interpolation between those groups is used as input for the SAIL model. This was done by adding a dynamic LIDF group 13 to the model, which is calculated in the following way:

If DaS ≤ 0.5\*S then

$$LIDF(13,i) = ((LIDF(9,i)*((0.5*S) - DaS) / (0.5*S)) + ((LIDF(2,i)*DaS) / (0.5*S)) \tag{13}$$

If DaS > 0.5\* S then

$$LIDF(13,i) = ((LIDF(2,i)*((0.5*S) - (DaS - 0.5* S))) / (0.5*S)) + ((LIDF(7,i)*(DaS - 0.5*S)) / (0.5* S)) \tag{14}$$

Where: DaS Days after Sowing  
 LIDF(group,angle) Leaf Angle Inclination frequency  
 S Season duration in days

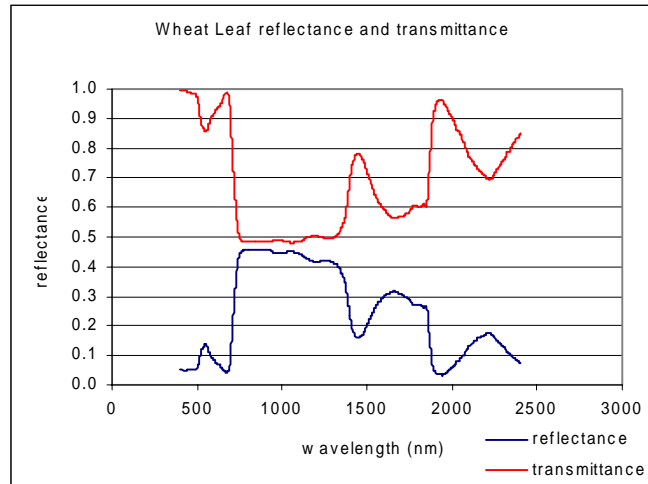


Figure 10: Laboratory reflectance and transmittance profile of wheat leaves.

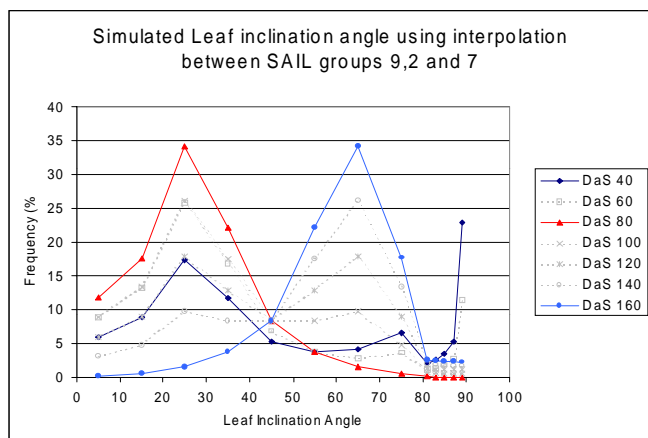


Figure 11: Simulated leaf inclination angle during the growing season.

Figure 11 shows how the LIDF changes during a simulated season of 160 days. At the first day we start with LIDF group 9 (erectophile) from SAIL, halfway the season at day 80 LIDF group 2 (planophile) is used and at the end of the season at day 160 group 7 is approached.

## 4 SENSITIVITY ANALYSIS

### 4.1 Introduction

The next paragraphs describe the effects of changing input parameters on both the combined CGI/SAIL model as well as the effects on the original SAIL model.

### 4.2 Soil Reflectance

*Soil brightness:* Overall reflectance increases with increasing soil reflectance. For the nadir CGI simulations we see that a local minimum appears at day 80 (default case in figure 12). Here we also find the hotspot peak reflectance. These peaks are caused by the amount of shadowed soil. From day 50 the crop height starts to grow fast, which causes the shadowing. However, this effect disappears after day 80 when the crop coverage reaches a point where it slowly starts to eliminate the effect of shadowing. *Shadow fraction:* SAIL is not influenced by shadowed soil reflection, also the hotspot CGI simulations are free from soil shadowing effects. The shadow fraction is used in the geometry model of the CGI nadir simulations. A decreasing shadowing fraction decreases the nadir CGI simulations. At low shadow fractions a local minimum appears near day 80.

#### 4.2.1 Crop Coverage

SAIL is not influenced by the crop coverage parameter. The coverage is calculated from the LAI values. Based on the coverage the crop diameter is calculated. We see that with an increasing coverage parameter the CGI simulations approach the SAIL simulations. However, hotspot peak reflectance and nadir local minimum for the CGI simulations still appear near day 80.

#### 4.2.2 Crop Height

*Maximum crop height:* SAIL is not influenced by crop height. Maximum crop height influences the height of the hotspot peak reflectance and the nadir local minimum near day 80. The lower the maximum crop height, the more the CGI model approaches the SAIL model. *Crop height breakpoint:* Lower breakpoint values causes the CGI reflection simulations to peak earlier in the season. Hotspot peak reflectance and nadir local minimum are more visible at low height breakpoints.

#### 4.2.3 Leaf Area Index

*Maximum LAI:* CGI hotspot simulations are slightly influenced by the maximum LAI values. However, CGI nadir simulations and both SAIL simulations increase with increasing maximum LAI values. *LAI breakpoint:* Hotspot peak reflectance shifts to the left with a lower LAI breakpoint. Also we see that this peak reflectance appears for the first time in the SAIL model. The LAI breakpoint determines at which place in time the LAI has had its maximum growth period.

#### 4.2.4 Sowing Day

Changing the sowing date with plus or minus 100 days has an enormous effect on the reflection behaviour. This is mostly caused by the changing sun angles during the season. However, minor changes such as 10 days won't influence the seasonal reflection very much.

## 5 RESULTS

A model as described above has been built in Visual Basic and is called CGI (Crop Geometry Interaction). Nadir and hotspot infrared wheat reflection POLDER measurements were isolated from the data set for the fields 101 and 300 of the ReSeDA test site. The flights were scheduled between 10:30 and 11:00 GMT. Unfortunately the first available POLDER flight was on day 82 after sowing, therefore it is not possible to compare the models with the early stages of the growing season. Although there were many view directions, there were not sufficient points to describe hotspot reflectance for field 101. For field 300 some hotspot points could be selected but in some cases we had to do with near hotspot measurements between +/- 10 degrees off-hotspot for azimuth or zenith angles. Within the limited amount of hotspot measurements for a given date and field there was a variation of 1 to 2.5 percent for most of the season.

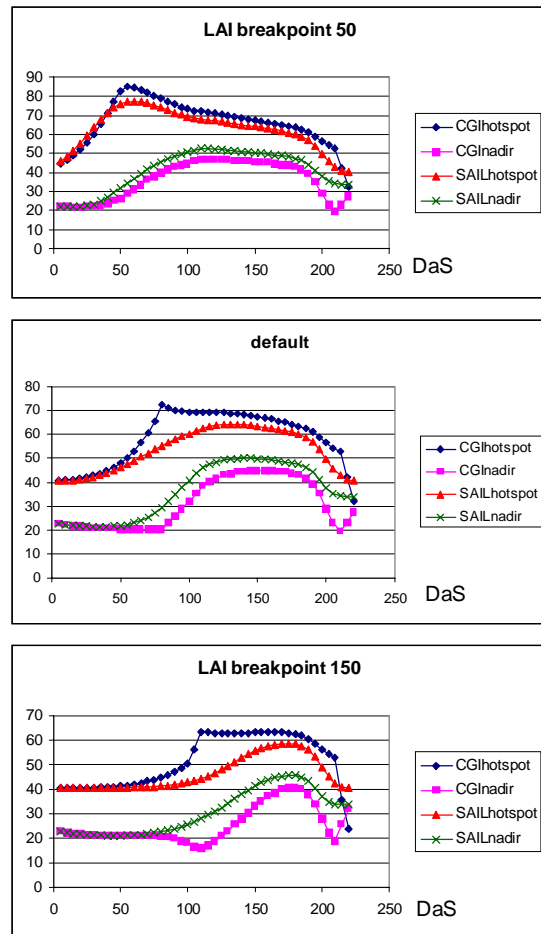


Figure 12: Sensitivity analysis for the LAI breakpoint value

However, the last day of measurements (212 days after sowing) had an average variation of  $\pm 10$  percent. This could be caused by weed.

Nadir reflection was simulated successfully using the CGI model, except for the last two measurements. Cause can be found in the exceptional early decrease in green LAI of field 300 compared to the other measured fields. Decrease of green LAI at field 300 started almost 50 days earlier.

For calibration of the hotspot reflection there is a need for more accurate hotspot measurements under field conditions. It was tried to find an index between nadir and hotspot infrared reflection that would yield a unique value for each day in the growing season. However, no such index was found yet. Most indices result in a peak value near day 80. The low sun position at this time of the year in combination with the crop height and diameter causes almost complete crop coverage when seen from the hotspot position. Results of the simulations versus the measurements can be found in figure 13.

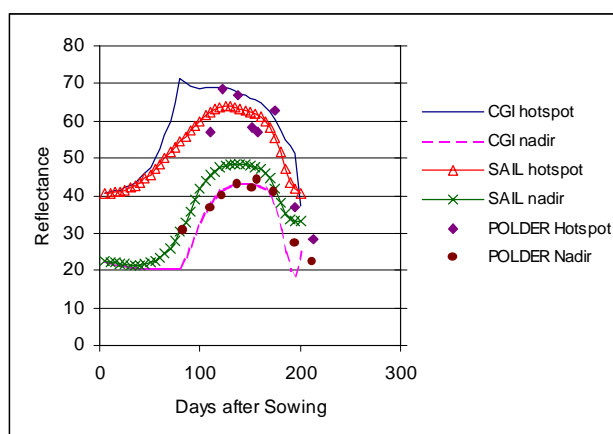


Figure 13: POLDER nadir and hotspot measurements versus seasonal simulations with SAIL and CGI

## 6 CONCLUSIONS

Total reflection is influenced by sun and view angles. Simulations show that total nadir infrared reflection is mostly influenced by soil properties in the first 90 days after sowing. Later on directional crop behaviour determined the total reflectance received by the sensor. High sun zenith angles (60-70) in the beginning of the year at the time of the POLDER measurements (10:40) eliminated the sunlit soil reflection in the hotspot already early in the season. Although crop reflection simulations seem successful with the SAIL and combined CGI/SAIL model, it was not succeeded to predict crop height or diameter using a combination of infrared nadir and hotspot images. Indices show no unique value that could be related to crop height or diameter. For improved calibration of the hotspot reflection there is a need for more accurate hotspot measurements under field conditions. Also there is a need for hotspot and nadir measurements in the first 80 days of the growing season. Future research could focus on the influence of viewing geometry in combination with visible reflection bands, or on the possibility of combining hotspot/nadir infrared reflectance indices with estimation of LAI using a combination of WdVI and the CLAIR model (Clevers 1991; Bouman et al. 1992).

## ACKNOWLEDGEMENTS

The ReSeDA project was funded by the EEC-DG XII (contract ENV4-CT96-0326 - PL952071). The *Laboratoire d'Optique Atmosphérique* (Lille, France) provided the POLDER airborne instrument.

## REFERENCES

- Bouman, B.A.M., H.W.J. van Kasteren, and D. Uenk, 1992. Standard relations to estimate ground cover and LAI of agricultural crops from reflectance measurements, *Eur. J. Agron.* 4:249-262.
- Buiten, H.J. and J.G.P.W. Clevers (ed), 1993. *Land Observation by Remote Sensing: Theory and Applications. Current Topics in Remote Sensing Volume 3.* Gordon and Breach science publishers. Amsterdam.
- Clevers, J.G.P.W., 1991. Application of the WdVI in estimating LAI at the generative stage of barley. *ISPRS Journal of Photogrammetry and Remote Sensing* 46: 37-47.
- Jacquemoud, S., F. Baret and J.F. Hanocq, 1992. Modeling Spectral and Bidirectional Soil Reflectance. *Remote Sensing of Environment* 41:123-132
- Nilson, T and U. Peterson, 1991. A Forest Canopy Reflectance Model and a Test Case. *Remote Sensing of Environment* 37:131-142
- Prévo, L., F. Baret, A. Olioso, J.P. Wigneron, J.G.P.W. Clevers et al., 1998. Assimilation of multi-temporal remote sensing data to monitor vegetation and soil: the Alpilles-ReSeDA project. *Proc. IGARSS '98 Symposium, July 1998, Seattle, WA, USA*, 3 pp.
- Rosema A., W. Verhoef, H. Noorbergen and J.J. Borgesius, 1992. A new forest light interaction model in support of forest monitoring. *Remote Sensing of Environment* 42:23-41
- Verhoef, W. and N.J.J. Bunnik, 1981. Influence of crop geometry on multispectral reflectance determined by the use of canopy reflectance models. *Proc. Int. Coll. On Signatures of Remotely Sensed Objects, Avignon, France*, pp. 273-290